Clinical validation of Venetoclax volumetric microsampling in patients with leukemia with assessment of whole-blood-to-plasma conversion strategies and self-microsampling feasibility

Levens, A.D.; Rijstenbil, J.; Metscher, E.; Borne, P. von dem; Albersen, A.; Swen, J.J.; Moes, D.J.A.R.

Clinical Pharmacokinetics
https://doi.org/10.1007/s40262-026-01635-3

ORIGINAL RESEARCH ARTICLE

Clinical Validation of Venetoclax Volumetric Microsampling in Patients with Leukemia with Assessment of Whole-Blood-to-Plasma Conversion Strategies and Self-Microsampling Feasibility

A. D. Levens[1] · J. Rijstenbil[1] · E. Metscher[1] · P. von dem Borne[2] · A. Albersen[3] · J. J. Swen[1] · D. J. A. R. Moes[1]

Received: 12 December 2025 / Accepted: 17 March 2026

Abstract

Background and Objective Venetoclax shows substantial pharmacokinetic (PK) variability and frequent toxicity, making it an archetypal candidate for PK monitoring. Capillary microsampling may facilitate decentralized PK monitoring of venetoclax. However, clinical validation is lacking. This study aimed to clinically validate capillary microsampling for venetoclax and to assess the feasibility of home-based self-microsampling.

Methods Adult patients with acute myeloid leukemia (AML) and chronic lymphocytic leukemia (CLL) receiving oral venetoclax therapy provided paired venous plasma and capillary samples using dried blood spot (DBS) and volumetric absorptive microsampling (VAMS) devices. We evaluated individualized hematocrit-based microsample-to-plasma correction models and previously published whole-blood-to-plasma conversion strategies. Agreement and predictive performance were assessed according to international microsampling validation criteria. The feasibility of home-based self-microsampling was evaluated by examining patients' ability to collect samples independently, the proportion of usable returned samples, and device usability.

Results A total of 25 patients contributed 64 sets of paired venous plasma, DBS, and VAMS samples. Uncorrected DBS and VAMS venetoclax concentrations underestimated plasma concentrations (mean bias −21% and −14%, respectively) and showed clear hematocrit dependence. Individualized hematocrit–plasma/microsample ratio models showed excellent performance, with 95% of DBS and 91% of VAMS concentrations within ±20% of plasma and low bias and imprecision across all validation metrics. Literature-based correction strategies showed lower acceptance rates and wider limits of agreement. Among patients attempting self-microsampling, 18 of 21 sampled independently, 76% of returned DBS/VAMS samples were suitable for analysis, and usability ratings were higher for VAMS than DBS.

Conclusions Capillary microsampling enables accurate venetoclax quantification in patients with AML and CLL when individualized hematocrit-based microsample-to-plasma conversion is applied. Both DBS and VAMS met international validation criteria, and home-based self-microsampling proved feasible. Venetoclax home-based self-microsampling warrants further study as a tool for decentralized PK monitoring.

1 Introduction

Venetoclax is a potent, selective B-cell lymphoma-2 (BCL-2) inhibitor that has transformed the treatment of hematological malignancies, including chronic lymphocytic leukemia (CLL) and acute myeloid leukemia (AML) [1]. Although substantial inter- and intra-individual pharmacokinetic (PK) variability has been documented, venetoclax dosing remains fixed after an initial ramp-up phase [2]. This variability may contribute to the wide range of adverse events observed in clinical practice, including neutropenia, febrile neutropenia, thrombocytopenia, diarrhea, infections, and nausea [3, 4]. In population PK analyses, the unexplained inter-patient variability in venetoclax clearance is approximately 40% [5]. Similarly, real-world data in patients with AML have shown highly variable trough concentrations (C_0) across studies [6, 7].

✉ D. J. A. R. Moes
d.j.a.r.moes@lumc.nl

[1] Department of Clinical Pharmacy and Toxicology, Leiden University Medical Center, Leiden, The Netherlands

[2] Department of Hematology, Leiden University Medical Center, Leiden, The Netherlands

[3] Department of Clinical Chemistry and Laboratory Medicine, Leiden University Medical Center, Leiden, The Netherlands

Published online: 22 April 2026

Key Points

Venetoclax quantification from capillary microsamples closely aligned with standard venous plasma concentrations.

Literature-based whole-blood-to-plasma correction factors performed inconsistently for venetoclax, indicating the need for drug-, device-, and population-specific calibration.

Home-based self-microsampling for venetoclax was feasible: most patients sampled independently, most returned samples were analytically adequate, and usability favored volumetric absorptive microsampling (VAMS) over dried blood spots (DBS) for decentralized pharmacokinetic monitoring.

The intra- and inter-patient PK variability arises from both intrinsic factors, including ethnicity and severe hepatic impairment [8], and sex [9], as well as clinical circumstances such as commonly occurring drug–drug interactions with rituximab, *CYP3A4* inhibitors, *OATP1B1* transporter inhibitors [9], *P-gp* and *BCRP* inhibitors [8], and food intake [9]. For instance, posaconazole, a strong *CYP3A4* inhibitor and common co-medication in AML treatment, increases venetoclax $AUC_{0–24}$ by ninefold [10], prompting substantial dose reductions that vary between regulatory agencies: the U.S. Food and Drug Administration (FDA) recommends 70 mg daily [11], while the European Medicines Agency (EMA) advises a maximum of 100 mg [2]. In addition to pharmacokinetic (PK) drug interactions, patient behavior also contributes to intra-individual PK variability. Taking venetoclax with high-fat meals can increase bioavailability up to fourfold, compared with fasting [9]. Collectively, these characteristics make venetoclax a compelling candidate for PK monitoring, as highlighted by pharmacokinetic drug–drug interaction and pharmacokinetic boosting studies [12, 13]. In practice, this is realized through therapeutic drug monitoring (TDM), which has become increasingly integrated into the standard of care for patients receiving oral oncolytic drugs [14].

Despite the growing role of TDM in oral oncolytic therapy, broader implementation may be limited by practical constraints. Conventional venous blood sampling requires hospital visits, trained personnel, and cold-chain logistics to maintain sample integrity. This can be burdensome for patients, particularly when frequent sampling is required. Moreover, venous sampling is invasive and resource intensive. Microsampling offers a promising alternative by enabling the collection of small blood volumes (typically less than 50 µL) through minimally invasive procedures that do not require trained phlebotomists. It allows for relatively simplified sample preparation, reduced biohazard risk, improved stability at room temperature, and easier transport and storage [15]. Microsampling could be particularly advantageous for patients with hematologic malignancies, who are often thrombocytopenic [16] and for whom venous sampling may pose additional challenges. These advantages may support more comprehensive and accurate PK assessments beyond trough levels while potentially reducing healthcare costs, enhancing accessibility, and empowering patients to take a more active role in their own treatment [17].

While microsampling offers promising advantages, it also presents methodological challenges related to physiological and compositional differences between capillary whole blood and venous plasma. These include preanalytical variability, such as sample collection, potential matrix effects, and the influence of hematocrit (Hct) and other blood composition parameters on measurement accuracy [18, 19]. The use of volumetric microsampling devices may help mitigate some of these challenges, though their impact requires evaluation within a clinical validation study. To date, several bioanalytical methods have been developed for microsampling of oncolytic drugs, yet only a limited number of studies have conducted clinical validation comparing microsampling to conventional venous blood sampling [18]. Such validation is essential before microsampling can be implemented in routine care [19]. Following clinical validation, the feasibility of home-based self-sampling must also be assessed to enable successful integration into clinical practice [20].

Comprehensive clinical validation of microsampling for venetoclax has not yet been reported. To address this gap, this study aimed to clinically validate a bioanalytical method for quantifying venetoclax concentrations in capillary blood using two patient-friendly volumetric microsampling devices. Both dried blood spot (DBS) and volumetric absorptive microsampling (VAMS) devices were included to allow comparison of venetoclax performance using two different microsampling techniques. In addition, we evaluated the feasibility of home-based self-microsampling with these devices in patients with AML and CLL receiving venetoclax therapy.

2 Methods

2.1 Study Population

This single-center, prospective clinical validation study was conducted at the Leiden University Medical Center (LUMC) between October 2024 and January 2025, in accordance with the principles of the Declaration of Helsinki. Ethical approval was obtained from the Medical Ethics Review Committee (reference NL86162.058.24). In line with International Association for Therapeutic Drug Monitoring and

Clinical Toxicology (IATDMCT) guideline, which recommend a minimum of 40 samples from at least 25 individual patients when patient numbers are limited [19], we aimed to include 25 adult patients. Eligible participants were 18 years of age or older, currently using venetoclax, and willing and able to provide written informed consent. No exclusion criteria were applied to reflect real-world clinical practice and assess the feasibility of microsampling under routine conditions. An overview of the study design is shown in Fig. 1.

2.2 Sample Collection

Sample collection for the clinical validation component was performed during routine venous blood draws by trained personnel and coincided with TDM of venetoclax. When trough sampling for TDM was not feasible due to timing constraints, blood was collected during routine follow-up instead. This allowed us to obtain paired microsamples and plasma samples across a wide concentration range, thereby supporting calibration at both high and low venetoclax levels. Immediately following venipuncture, capillary blood was collected via finger-prick on the basis of the microsampling protocol routinely used in clinical care for organ transplant patients at the LUMC [21].

Finger-pricks were performed by study investigators (J.R. and A.D.L.) using a safety lancet (Sarstedt, Nümbrecht, Germany). After discarding the first drop of blood, capillary blood was collected for both DBS and VAMS. DBS sampling was performed using the HemaXis DB10 device, which utilizes integrated capillaries to apply 10 µL volume onto a Whatman 903 protein saver filter card (DBS System, Gland, Switzerland). An additional 10 µL of capillary blood was obtained using the volumetric absorptive microsampling (VAMS) Mitra Clamshell device (Neoteryx, Torrance, CA, USA), which collects a fixed volume through an absorptive porous tip. Samples were collected at a minimum of 4 days after treatment initiation to ensure venetoclax concentrations were at steady state (clinically relevant concentration range) on the basis of its reported half-life of approximately 14–26 h [22, 23]. The timing of venipuncture, DBS, and VAMS sampling, as well as the time of the most recent venetoclax administration, was recorded on a standardized form by the study investigators. To ensure compliance with IATDMCT recommendations, venous and capillary samples were collected within a 0–10 min window of each other [19]. Following collection, DBS and VAMS samples were dried at room temperature for a minimum of 24 h before being stored at − 80 °C until bioanalysis.

2.3 Bioanalysis

All DBS and venous plasma samples were analyzed using liquid chromatography-tandem mass spectrometry (LC-MS/MS) at the ISO 15189-accredited laboratory of the department of Clinical Pharmacy & Toxicology of the LUMC. A validated multi-analyte LC-MS/MS assay, capable of quantifying venetoclax in DBS and VAMS samples, was used for the analysis. This assay was developed and validated in accordance with the International Council for Harmonization Guideline M10 on Bioanalytical Method Validation and Study Sample Analysis [24]. The validated analytical range for venetoclax quantification was 50–5000 µg/L.

2.4 DBS and VAMS to Plasma Correction Strategies

Physiological differences between capillary whole blood (as sampled with DBS or VAMS) and venous plasma can introduce systematic discrepancies in measured drug concentration, particularly for analytes that do not partition into red blood cells [19]. Venetoclax is highly protein-bound (unbound fraction $fu < 0.01$), does not distribute into the erythrocyte compartment of blood ($Kbc/pla \approx 0$), and has a reported mean blood-to-plasma concentration ratio (Fp, also referred to as Kb/p) of 0.57 [5, 22]. Consequently, when measured in capillary whole blood via DBS or VAMS, venetoclax concentrations may appear lower than corresponding plasma concentrations, reflecting the smaller plasma fraction at higher Hct values. For this reason, we recorded Hct levels closest to the day of paired sampling, as well as Hct sampling intervals. In addition, Hct coefficients of variation (CV) were calculated from all Hct measurements within the year preceding sampling to capture individual variability over time. As the primary whole-blood-to-plasma correction strategy, we used the observed relationship between Hct and the plasma-to-microsample concentration ratio to adjust microsample concentrations. In addition, we assessed conversion strategies described in the literature for translating microsample measurements to plasma-equivalent values of oncolytic drugs. Our evaluation focused on compounds that partition predominantly into plasma, such as venetoclax [25]. These approaches incorporate Hct values, drug-specific distribution parameters, or empirical methods, using correction factors or regression formulas, and were evaluated for their ability to improve agreement with venous plasma reference concentrations. A concise overview of the correction strategies included in our evaluation is provided in Table 1, whereas a comprehensive description of all reviewed methods, their underlying assumptions, and reported acceptance rates (AR) is available in Supplementary Table S1 to contextualize our findings.

2.5 Self-Sampling Feasibility

To assess the feasibility of self-microsampling by patients, patients received a kit (HemaXis DB10, Mitra Clamshell, safety lancets, written instructions, intake/collection log,

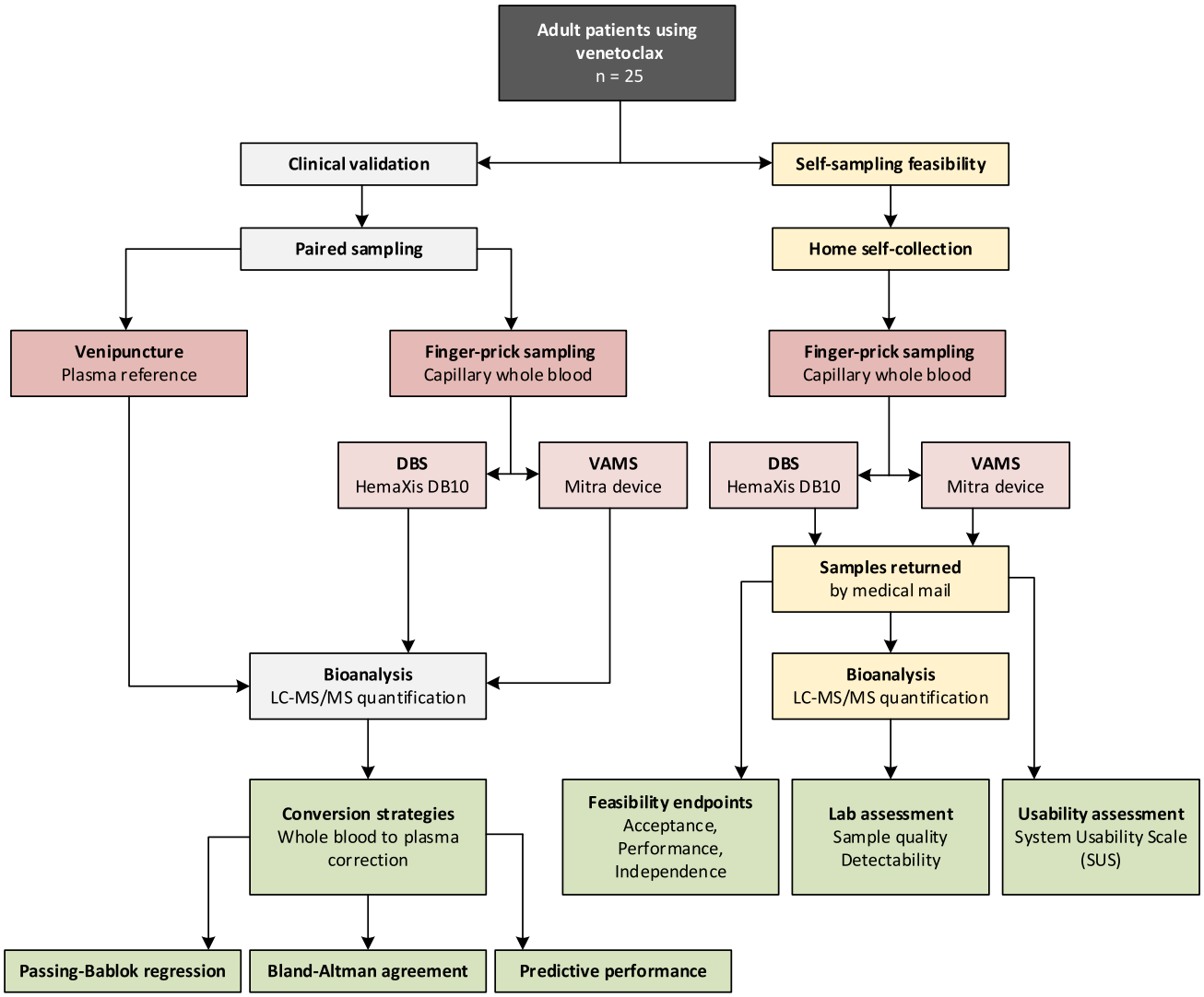

Fig. 1 Schematic overview of the study design. The study consisted of two complementary components: (i) clinical validation of capillary microsampling for venetoclax quantification and (ii) assessment of the feasibility of patient-performed home microsampling. For the clinical validation component, adult patients receiving venetoclax underwent paired sampling during routine clinical visits, consisting of venous blood collection (venipuncture; plasma reference) and finger-prick sampling (capillary whole blood). Capillary samples were collected using DBS (HemaXis DB10) and VAMS (Mitra device). Venetoclax concentrations were quantified by LC–MS/MS. Agreement between microsampling-derived and plasma concentrations was evaluated using Passing–Bablok regression, Bland–Altman analysis, and predictive performance metrics. Correction strategies to adjust whole-blood microsample concentrations to plasma-equivalent values were subsequently evaluated. For the self-sampling feasibility component, patients performed home-based microsampling using DBS and VAMS samples collected by finger-prick and returned by medical mail. Feasibility was evaluated through predefined endpoints (acceptance, performance, and independence), laboratory assessment of returned samples (sample quality and detectability), and usability evaluation of both microsampling devices using the System Usability Scale. *DBS* dried blood spot, *VAMS* volumetric absorptive microsampling, *LC-MS/MS* liquid chromatography-tandem mass spectrometry

prepaid return envelope) adapted from a routine clinical microsampling protocol [21]. Patients were instructed to collect duplicate samples using both devices and return all four samples by post within 1 week. Upon receipt, a laboratory technician evaluated sample quality using predefined criteria. For DBS, quality issues included insufficient sample volume, no capillary filling, incomplete capillary emptying, material placed outside the designated spot, or excessive sample volume. For VAMS, quality issues included oversampling or incomplete tip filling. DBS and VAMS samples were also analyzed to confirm the detectability of venetoclax.

Table 1 Overview of literature-based correction strategies for translating dried blood spot (DBS) or volumetric absorptive microsampling (VAMS) concentrations to plasma-equivalent values, and their reported outcomes across different drugs. These strategies were reviewed and subsequently applied to venetoclax in the present study.

Correction strategy	Equation no.	Equation used	Analyte	Source study
Hematocrit–plasma/capillary ratio (linear model)	(1a)	$EC_{\text{plasma}} = C_{\text{cap}} \times (a \times Hct + b)$	Venetoclax	Current study
Hematocrit–plasma/capillary ratio (exp model)	(1b)	$EC_{\text{plasma}} = C_{\text{cap}} \times (a \times e^{(b \cdot Hct)})$	Venetoclax	Current study
Hematocrit–plasma/capillary ratio (log model)	(1c)	$EC_{\text{plasma}} = C_{\text{cap}} \times (a \times \ln(Hct) + b)$	Venetoclax	Current study
Hematocrit–plasma/capillary ratio (polynomial model)	(1d)	$EC_{\text{plasma}} = C_{\text{cap}} \times ((a \times Hct) + (b \times (Hct)^2 + c)$	Venetoclax	Current study
Hematocrit (individual or mean) and blood-to-plasma partitioning	(2a)	$EC_{\text{plasma}} = \frac{C_{\text{cap}}}{(1 - Hct) + Hct \times \rho \times f_u}$	Nilotinib	Boons et al. (2017) [26]
	(2b)	$EC_{\text{plasma}} = \frac{C_{\text{cap}}}{(1 - Hct) + K \frac{bc}{pla} \times Hct}$	Tamoxifen and (Z)-endoxifen	Jager et al. (2014) [27]
			Vemurafenib	Nijenhuis et al. (2016) [28]
	(2c)	$EC_{\text{plasma}} = \frac{C_{cap}}{(1 - Hct)} \times F_p$	Imatinib	Antunes et al. (2015) [29]
			Irinotecan and SN-38	Hahn et al. (2018) [30]
			Paclitaxel	Andriguetti et al. (2018) [31]
			Docetaxel	Raymundo et al. (2018) [32]
Hematocrit (individual, mean, or fixed)	(3a)	$EC_{\text{plasma}} = \frac{C_{\text{cap}}}{\left(1 - Hct_{individual}\right)}$	Imatinib, dasatinib, and nilotinib	Kralj et al. (2012) [33]
			Etoposide	Kukec et al. (2016) [34]
			Imatinib and norimatinib	Iacuzzi et al. (2019) [35]
	(3b)	$EC_{\text{plasma}} = \frac{C_{\text{cap}}}{\left(1 - Hct_{\text{mean}}\right)}$	Venetoclax	Current study
	(3c)	$EC_{\text{plasma}} = \frac{C_{\text{cap}}}{\left(1 - Hct_{\text{fixed}}\right)}$	Pazopanib	De Wit et al. (2015) [36]
	(3d)	$EC_{\text{plasma}} = \frac{C_{\text{cap}}}{\left(1 - Hct + Hct^2\right)}$	Radotinib	Lee et al. (2020) [37]
Hematocrit (individual) and experimentally determined correction factor	(4)	$CF = \frac{C_{\text{cap}}}{C_{\text{plasma}}}$	Tamoxifen and three metabolites	Antunes [38]
		$EC_{\text{plasma}} = \frac{C_{\text{cap}}}{\left(1 - Hct_{\text{individual}}\right)} \times CF$	Docetaxel	Raymundo et al. (2018) [32]
On the basis of experimentally determined correction factor (per patient or per sample)	(5a)	$CF_{\text{patient}} = \frac{C_{\text{cap}}}{C_{\text{plasma}}}$	Imatinib	Antunes et al. (2015) [29]
		$EC_{\text{plasma}} = C_{\text{DBS}} \times CF_{\text{patient}}$	Irinotecan and SN-38	Hahn et al. (2018) [30]
			Paclitaxel	Andriguetti et al. (2018) [31]
			Imatinib and norimatinib	Iacuzzi et al. (2019) [35]
	(5b)	$EC_{\text{plasma}} = C_{\text{cap}} \times CF_{\text{sample}}$	Venetoclax	Current study
Deming or Passing–Bablok regression-derived calibration equation between plasma and capillary samples	(6a)	$EC_{\text{plasma}} = \frac{C_{\text{cap}} + b_{\text{Deming}}}{a_{(\text{Deming}(cap \sim plasma))}}$	Radotinib	Lee et al. (2020) [37]
			Nilotinib	Boons et al. (2017) [26]
			Pazopanib	Verheijen et al. (2016) [39]
	(6b)	$EC_{\text{plasma}} = \frac{C_{\text{cap}} + b_{\text{Passing-Bablok}}}{a_{(Passing-Bablok(cap \sim plasma)}}$	Venetoclax	Current study
	(6c)	$EC_{\text{plasma}} = \frac{C_{\text{cap}}}{a_{(Passing-Bablok(cap \sim plasma))}}$	Venetoclax	Current study
Linear regression between plasma and capillary	(7a)	$EC_{\text{plasma}} = a_{\text{cap}\sim\text{plasma}} \times C_{\text{cap}}$	Vemurafenib	Nijenhuis et al. (2016) [28]
	(7b)	$EC_{\text{plasma}} = a_{\text{cap}\sim\text{plasma}} \times C_{\text{cap}} + b$	Irinotecan and SN-38	Hahn et al. (2018) [30]
			Paclitaxel	Andriguetti et al. (2018) [31]

cap capillary, *CF* correction factor, *EC_plasma* estimated plasma concentration, *Fp* blood-to-plasma concentration ratio, *fu* unbound fraction, *Hct* hematocrit, *Kbc/pl* blood cell-to-plasma partition coefficient, *ρ·fu* red-blood-cell-to-unbound plasma ratio multiplied by unbound fraction

2.6 Statistical Analysis

Method comparison between DBS/VAMS and venous plasma followed the recently published IATDMCT guidance for converting capillary blood to plasma [40]. Passing–Bablok regression was used to assess the correlation between methods, accounting for variability in both test and reference samples [41]. Method agreement and potential bias were further evaluated using Bland–Altman analysis [42]. The span of the 95% limits of agreement (LoA) obtained from Bland–Altman analysis was compared with a predefined acceptance threshold of 25%. This threshold was selected on the basis of recommended venetoclax dose modification steps of at least 25% in case of toxicity [2] and supported by residual unexplained variability in venetoclax plasma concentrations reported in population PK models (48% CV residual error) [43], which exceeds this margin. Predictive performance was assessed by calculating the median percentage predictive error (MPPE) and the median absolute percentage predictive error (MAPE), with values $< 15\%$ considered clinically acceptable [40]. In addition, the root mean squared error (RMSE) and root mean squared percentage error (RMSPE) were reported as complementary measures of overall predictive error magnitude, in line with prior recommendations [18]. Acceptable agreement should be at least 67% of paired samples falling within 20% of the mean concentration [19].

Feasibility endpoints were predefined as follows: acceptance (enrolled patients who consented to self-microsampling), performance (consenting patients who attempted sampling), independence (attempts completed without caregiver assistance), and sample adequacy (returned DBS/VAMS meeting laboratory quality criteria and containing detectable venetoclax). Reasons for inadequacy were recorded. As part of feasibility, usability was evaluated using the System Usability Scale (SUS), a validated tool to assess end users' perceived ease of use and user friendliness [44]. The SUS consists of ten items rated on a 5-point Likert scale (1 = "strongly disagree" to 5 = "strongly agree"). Negatively worded items were reverse-scored, item scores were summed, and the total was multiplied by 2.5 to yield a 0–100 total, with higher scores indicating greater usability. Paired total SUS scores (0–100) were compared with the Wilcoxon signed-rank test, reporting the Hodges–Lehmann within-patient difference with 95% CI and p value ($\alpha = 0.05$, two-sided).

All analyses were performed in R 4.2.2 (R Foundation for Statistical Computing) with RStudio 2024.04.2. Core packages included *dplyr*, *ggplot2*, *patchwork*, *mcr*, and *MethComp*. MPPE, MAPE, RMSE, and RMSPE were calculated as:

$$MPPE = \frac{1}{n}\sum_{i=1}^{n}\frac{T_i - R_i}{R_i} \times 100$$

$$MAPE = \frac{1}{n}\sum_{i=1}^{n}\left|\frac{T_i - R_i}{R_i}\right| \times 100$$

$$RMSE = \sqrt{\frac{1}{n}\sum_{i=1}^{n}\left(T_i - R_i\right)^2}$$

$$RMSPE = \sqrt{\frac{1}{n}\sum_{i=1}^{n}\left(\frac{T_i - R_i}{R_i} \times 100\right)^2}$$

where T_i is the test method (DBS or VAMS) and R_i the reference (plasma) concentration.

3 Results

3.1 Patients and Samples

A total of 25 patients participated in this study. The median age was 69 years (range 21–84 years), with a majority of male patients (64%) and a mean Hct level of 0.34 L/L (SD 0.08). Patients received venetoclax at doses of 70 mg, 100 mg, 200 mg, or 400 mg as part of routine treatment for AML or CLL; 16 patients (64%) received posaconazole or voriconazole as concomitant medication during the study period. Further details on patient characteristics, treatment regimens, and sampling distributions are provided in Table 2. In total, 69 sets of paired venous plasma, DBS, and VAMS samples were collected across all participants. Five paired samples were excluded from analysis: one due to missing labeling and four because the time interval between plasma and capillary sampling exceeded the 10-min protocol-defined limit. As a result, 64 complete sets of paired venetoclax samples (DBS, VAMS, and plasma) were included in the final analysis. For most included samples, the Hct sampling interval was ≤ 1 day; samples with longer intervals were retained because within-patient Hct variability (CV) was low ($\leq 10\%$).

3.2 DBS and VAMS Versus Plasma Without Correction

Venetoclax concentrations ranged from 115 to 4508 µg/L in plasma, 84 to 4719 µg/L in DBS, and 103 to 4722 µg/L in VAMS. For DBS, Bland–Altman analysis showed a mean bias of −21% (95% CI −27 to −15) with 95% LoA

Table 2 Patient characteristics, venetoclax treatment regimens, concomitant medications, number of samples collected, and sampling timepoints for patients with complete sets of paired venous plasma, DBS, and VAMS samples

Pt	Age (years)	Sex	Diagnosis	Hct (L/L)	Hct-sampling interval (days)*	Hct CV (%)	Venetoclax dose	*CYP3A4* inhibitor	Combined treatment cycles	Paired samples	Sampling timepoints
1	73	Male	AML	0.394	20–21	8	400 mg	–	C23 Decitabine	4	T_0, T_1, T_3, T_4
2	80	Male	AML	0.257	0–1	15	100 mg	PCZ 300 mg	C3 Azacitidine	3	T_{5a}, T_{5b}, T_6
3	76	Female	AML	0.273	0–1	15	100 mg	PCZ 300 mg	C4 Azacitidine	2	T_6, T_7
4	77	Male	AML	0.447	2	4	400 mg	–	C3 Obinutuzumab	4	T_0, T_1, T_2, T_3
5	65	Female	AML	0.340	0–1	14	100 mg	PCZ 300 mg	C2 Azacitidine	2	T_0, T_6
6	69	Female	AML	0.277	0–1	13	100 mg	VCZ 800 mg	C3 Azacitidine	2	T_{14}, T_{16}
7	32	Male	AML	0.376	0–1	30	100 mg	PCZ 300 mg	C6 Azacitidine	4	T_0, T_1, T_7, T_8
8	76	Male	AML	0.451	2	6	100 mg	PCZ 200 mg	C12 Azacitidine	1	T_8
9	72	Male	AML	0.285	0–1	12	70 mg	PCZ 300 mg	C1 Azacitidine	4	T_0, T_1, T_3, T_4
10	68	Female	AML	0.232	0	12	70 mg	PCZ 300 mg	C1 Azacitidine	1	T_8
11	82	Male	AML	0.435	3–4	10	100 mg	PCZ 200 mg	C22 Decitabine	4	T_0, T_1, T_3, T_4
12	62	Male	AML	0.284	0	19	70 mg	PCZ 600 mg	C6 Azacitidine	4	T_0, T_1, T_5, T_6
13	84	Male	AML	0.291	0–1	6	100 mg	PCZ 300 mg	C2 Azacitidine	3	T_0, T_3, T_5
14	82	Male	AML	0.353	0	3	400 mg	–	C54 Decitabine	2	T_{20}, T_{21}
15	78	Female	AML	0.424	5–6	6	400 mg	–	C26 Decitabine	4	T_0, T_1, T_6, T_7
16	77	Female	AML	0.219	0–1	11	70 mg	PCZ 300 mg	C2 Azacitidine	4	T_0, T_1, T_5, T_6
17	72	Male	CLL	0.406	0–7	5	200 mg	–	–	2	T_1, T_5
18	27	Male	AML	0.259	0	24	70 mg	PCZ 300 mg	–	1	T_0
19	68	Female	CLL	0.388	0	18	400 mg	–	–	1	T_0
20	53	Male	AML	0.417	0–1	9	70 mg	PCZ 300 mg	C3 Decitabine	4	T_0, T_1, T_2, T_4
21	29	Male	AML	0.396	0	26	100 mg	PCZ 300 mg	C1 Azacitidine	2	T_0, T_6
22	21	Female	AML	0.302	0	20	400 mg	–	C1 Azacitidine	2	T_0, T_4
23	61	Male	CLL	0.491	0	4	400 mg	–	–	2	T_0, T_1
24	69	Male	AML	0.223	0	16	100 mg	VCZ 400 mg	C1 Azacitidine	1	T_4
25	69	Female	CLL	0.317	0	3	300 mg	–	–	1	T_0

pt patient, *AML* acute myeloid leukemia, *CLL* chronic lymphocytic leukemia, *Hct* hematocrit, *CV* coefficient of variation, *CYP3A4* cytochrome P450 3A4, *PCZ* posaconazole, *VCZ* voriconazole, *C* cycle, *DBS* dried blood spot, *VAMS* volumetric absorptive microsampling, *T* time after venetoclax ingestion (in h), *T5a, T5b* repeated T5 samples collected on separate days

*Values separated by a dash indicate distinct sampling days

from − 65% to 29%. Passing–Bablok regression yielded an intercept of − 106 (95% CI −149 to −62) and a slope of 1.027 (95% CI 0.878–1.198). Only 53% of samples were within 20% of mean concentration, with MPPE and MAPE of −13% and 19%, respectively. For VAMS, the mean bias was − 14% (95% CI − 18 to −10), with LoA from − 46% to 17%. Passing–Bablok regression gave an intercept of − 67 (95% CI − 104 to − 30) and a slope of 0.963 (95% CI 0.854–1.070). In this case, 64% of samples fell within 20%, with MPPE and MAPE of − 12% and 14%, respectively.

3.3 Hematocrit Effect

Given the suboptimal agreement between venetoclax concentrations obtained from DBS or VAMS and those from plasma, the potential impact of Hct was evaluated. For each sampling technique, the plasma-to-microsample ratio was plotted against Hct (Fig. 2). For DBS (Fig. 2a), the ratio correlated strongly with Hct ($R^2 = 0.71$). The slope of 3.52 reflected a steep increase, showing that higher values substantially inflated plasma/DBS ratios. For VAMS (Fig. 2b), the correlation was weaker ($R^2 = 0.37$), and the slope of 1.51 reflected a more modest effect, with plasma/VAMS ratios less influenced by Hct. Other monotonic models (polynomial, exponential, and logarithmic fits) were also evaluated, which yielded comparable coefficients of determination within each sampling technique (DBS: $R^2 =$ 0.70–0.72; VAMS: $R^2 = 0.34$–0.40; Supplementary Figs. S1 and S2).

3.4 Performance of Correction Methods for Estimating Plasma Concentrations from DBS

Application of the Hct-plasma/DBS ratio relationship provided the highest level of agreement with venetoclax plasma concentrations. The linear model (Eq. 1a) achieved an AR of 95% (61 of 64 samples within 20% of the mean concentration). MPPE was − 2.6%, MAPE 7.8%, with RMSE 167 µg/L and RMSPE 14%. Consistent with these metrics, the Bland–Altman plot shows a mean bias close to zero with 95% LoA around − 24% to 26%, mostly within the 25% band (Fig. 3a), and the Passing–Bablok calibration lies close to

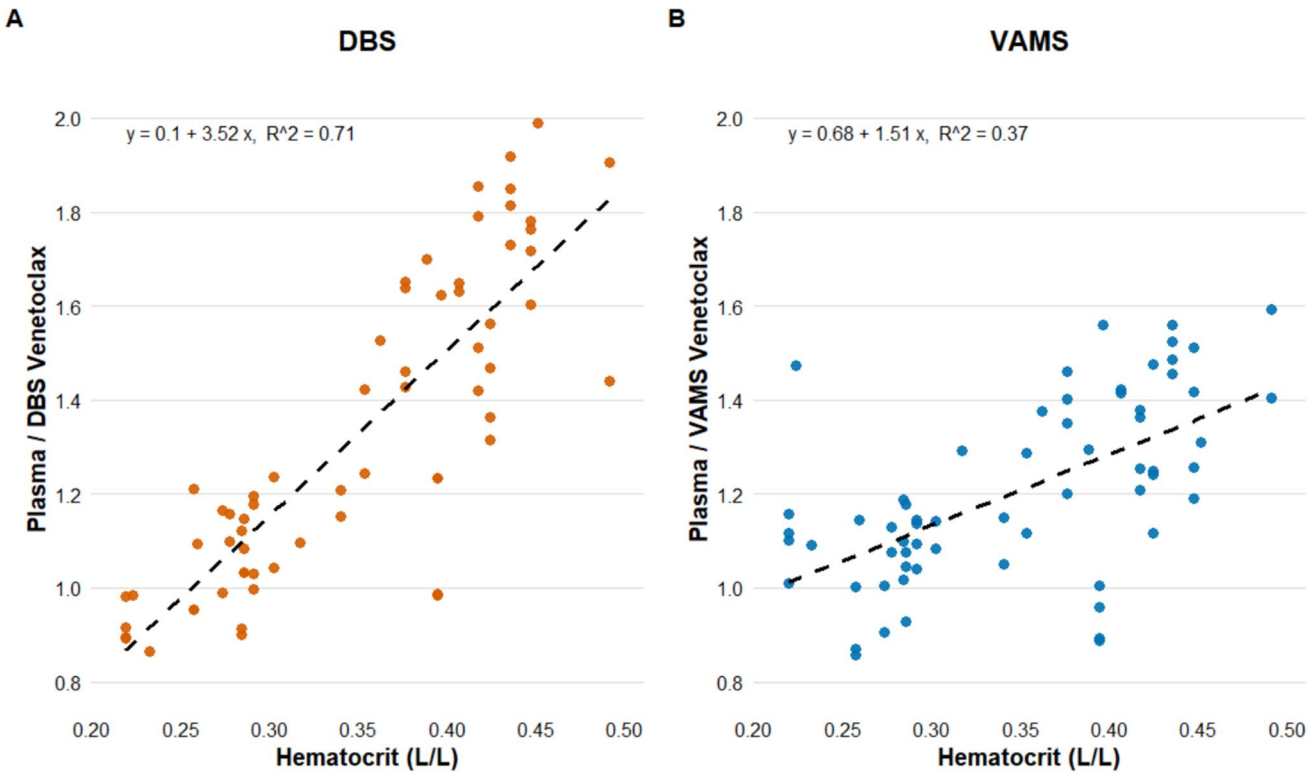

Fig. 2 Relationship between hematocrit and plasma-to-microsample concentration ratios of venetoclax. (**a**) Plasma/DBS ratio: each point represents a paired plasma and DBS sample from an individual measurement, using the hematocrit value recorded closest to sampling. The regression line is described by the equation: plasma/DBS venetoclax ratio = 0.10 +3.52 × hematocrit ($R^2 = 0.71$). (**b**) Plasma/VAMS ratio: each point represents a paired plasma and VAMS sample from an individual measurement, using the hematocrit value recorded closest to sampling. The regression line is described by the equation: plasma/VAMS venetoclax ratio = 0.68 + 1.51 × hematocrit ($R^2 =$ 0.37). Dashed lines indicate fitted regression lines

the identity line ($y = x$) with a small intercept (Fig. 3c). Other monotonic models (Eqs. 1b–d) yielded similar results. Notably, two of the three samples outside the acceptance range originated from a single patient whose Hct was measured more than 20 days apart from the corresponding sampling occasions (Table 2). Of note, the Hct CV was low (8%).

Among the literature-based correction strategies, a second tier of methods achieved AR values between 53 and 62%. This group included regression-based calibration approaches between DBS and observed plasma, namely ordinary linear regression (Eq. 7b), Deming regression (Eq. 6a), Passing–Bablok regression (Eq. 6b), and slope-only regressions (Eq. 6c, 7a), as well as a Hct-adjusted correction (Eq. 3d). These approaches showed higher error (MAPE 15–20%) and wider LoA (up to 65%), with evidence of proportional bias (0.929–1.200). The poorest-performing strategies were those based on empiric multipliers rather than fitted relationships (Eq. 2c, 4, 5a, 5b). These approaches achieved AR values as low as 11%, with high bias and wide LoA, in most cases performing worse than when no correction strategy was applied. Detailed results for all correction strategies are provided in Table 3.

3.5 Performance of Correction Methods for Estimating Plasma Concentrations from VAMS

Compared with DBS, the best-performing VAMS correction models achieved slightly lower agreement with plasma (91% versus 95%), yet a greater number of correction strategies met the predefined 67%/20% AR. The linear model (Eq. 1a) yielded an AR of 91% (58 of 64 samples within 20% of the mean concentration), MPPE close to zero (− 0.1%), MAPE of 8.2%, with RMSE 234 µg/L and RMSPE 14%. In line with these results, the Bland–Altman plot shows no significant mean bias with 95% LoA near − 25% to 27% (Fig. 3b), and the Passing–Bablok fit has a slope near unity and negligible intercept, tracking the identity line ($y = x$) (Fig. 3d). Other monotonic fits (Eq. 1b, 1c, 1d) performed similarly, with AR values of 88–91% and comparably low error metrics. Again, the same patient (Hct sampling interval 20–21 days; Hct CV 8%) who contributed two out-of-range samples in DBS was also responsible for all four out-of-range samples in VAMS.

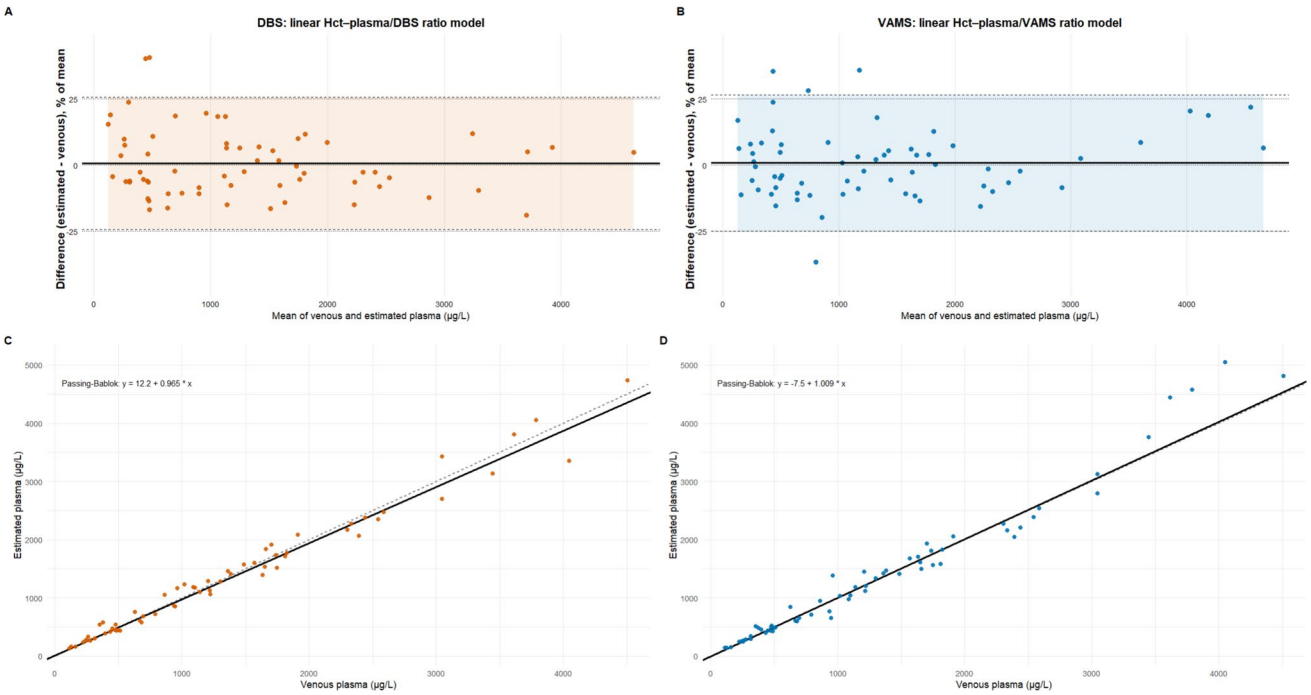

Fig. 3 Agreement and calibration of microsampling-derived venetoclax concentrations against venous plasma. (**a**–**b**) Bland–Altman plots for DBS and VAMS using a linear hematocrit-plasma/method ratio model to estimate plasma. Points are percentage difference versus method mean; the solid line is the mean bias and dashed lines are the 95% limits of agreement; pale bands indicate the limits-of-agreement region; dotted lines mark ±25% acceptance. (**c**–**d**) Passing–Bablok regressions of DBS- and VAMS-estimated plasma versus venous plasma; the solid line is the Passing-Bablok fit with the equation printed on the panel; the grey dashed line is the identity ($y = x$). Axes are harmonized within each row for visual comparability. *BA* Bland–Altman, *DBS* dried blood spot, *VAMS* volumetric absorptive microsampling, *Hct* hematocrit, *PaBa* Passing–Bablok, *LoA* limits of agreement, *ULA* upper limit of agreement, *LLA* lower limit of agreement

Table 3 Performance of correction methods for estimating plasma-equivalent venetoclax concentrations from DBS measurements. Methods are ranked by acceptance rate (percentage of samples with predicted plasma concentration within 20% of the mean concentration)

Correction strategy	Equation no.	Equation	AR (%)	*n* accept	*n* reject	MPPE (%)	MAPE (%)	RMSE (µg/L)	RMSPE (%)	Mean bias (95% CI, %)	95% LoA (%, lower–upper)	Proportional bias	Constant bias
Hematocrit-plasma/capillary ratio (linear model)	(1a)	$EC_{\text{plasma}} = C_{DBS} \times (a \times Hct + b)$	95	61	3	−2.6	7.8	167	14	0.7 (−2.5 to 3.9)	−24 to 26	0.965	12
Hematocrit-plasma/capillary ratio (exp model)	(1b)	$EC_{\text{plasma}} = C_{DBS} \times (a \times e^{(b \cdot Hct)})$	95	61	3	−0.9	7.6	183	15	0.8 (−2.3 to 3.9)	−24 to 25	0.974	5
Hematocrit-plasma/capillary ratio (log model)	(1c)	$EC_{\text{plasma}} = C_{DBS} \times (a \times \ln(Hct) + b)$	95	61	3	−1.7	8.6	162	14	0.7 (2.7–4.0)	−26 to 27	0.965	19
Hematocrit-plasma/capillary ratio (polynomial model)	(1d)	$EC_{\text{plasma}} = C_{DBS} \times ((a \times Hct) + (b \times (Hct)^2 + c)$	95	61	3	−1.6	7.8	162	14	0.7 (−2.4 to 3.9)	−24 to 25	0.971	10
Plasma-capillary calibration (linear regression)	(7b)	$EC_{\text{plasma}} = a \times C_{DBS} + b$	62	40	24	4.2	15	251	38	7.5 (0.8–14.2)	−45 to 60	0.929	121
Plasma-capillary calibration (Deming regression)	(6a)	$EC_{\text{plasma}} = \frac{C_{DBS}+b}{a_{DBS\sim plasma}}$	61	39	25	3.7	15	253	32	5.5 (−0.8 to 12)	−44 to 55	0.957	85
Plasma-capillary calibration (Passing–Bablok regression)	(6b)	$EC_{\text{plasma}} = \frac{C_{DBS}+b}{a_{DBS\sim plasma}}$	61	39	25	0.1	17	265	22	−2.3 (−7.8 to 3.1)	−45 to 40	1.001	−0.7
Plasma-capillary calibration (slope Passing–Bablok regression)	(6c)	$EC_{\text{plasma}} = \frac{C_{DBS}}{a_{DBS\sim plasma}}$	55	35	29	16	16	294	26	−21 (−27 to −15)	−67 to 26	1.001	−103

Table 3 (continued)

Correction strategy	Equation no.	Equation	AR (%)	*n* accept	*n* reject	MPPE (%)	MAPE (%)	RMSE (µg/L)	RMSPE (%)	Mean bias (95% CI, %)	95% LoA (%, lower–upper)	Proportional bias	Constant bias
Hematocrit (individual)	(3d)	$EC_{\text{plasma}} = \frac{C_{DBS}}{(1 - Hct + Hct^2)}$	53	34	30	4.7	20	378	22	−0.1 (−5.5 to 5.3)	−43 to 43	1.200	−106
Plasma-capillary calibration (slope linear regression)	(7a)	$EC_{\text{plasma}} = \frac{C_{DBS}}{a_{DBS\sim plasma}}$	53	34	30	−13	19	290	25	−18 (−24 to −12)	−65 to 29	1.027	−106
Hematocrit (individual)	(3a)	$EC_{\text{plasma}} = \frac{C_{DBS}}{(1 - Hct_{\text{individual}})}$	52	33	31	21	21	525	29	18 (14–22)	−12 to 48	1.306	−53
Hematocrit (individual) and blood-plasma partitioning (Kbc/pla)	(2b)	$EC_{\text{plasma}} = \frac{C_{DBS}}{(1 - Hct) + K\frac{bc}{pla} \times Hct_{\text{individual}}}$	52	33	31	21	21	529	29	18 (14–22)	−12 to 48	1.306	53
Hematocrit (individual) and blood-plasma partitioning ($\rho \times f_u$)	(2a)	$EC_{\text{plasma}} = \frac{C_{DBS}}{(1 - Hct) + Hct_{\text{individual}} \times \rho \times f_u}$	52	33	31	21	21	525	29	18 (15–22)	−12 to 48	1.310	−55
Correction factor (patient level)	(5a)	$EC_{\text{plasma}} = C_{DBS} \times CF_{\text{patient}}$	48	31	33	−7.3	20	313	23	−12 (−18 to −6)	−59 to 36	1.099	−114
No correction strategy	–	–	48	31	33	−19	19	310	28	−25 (−31 to −19)	−71 to 22	0.960	−98
Correction factor (sample level)	(5b)	$EC_{\text{plasma}} = C_{DBS} \times CF_{\text{sample}}$	47	30	34	0.0	22	389	23	−4.1 (−10 to 2.0)	−51 to 43	1.194	−129
Hematocrit (mean)	(3b)	$EC_{\text{plasma}} = \frac{C_{DBS}}{(1 - Hct_{\text{mean}})}$	41	26	38	24	24	786	37	17 (11–23)	−30 to 64	1.489	−164
Hematocrit (fixed)	(3c)	$EC_{\text{plasma}} = \frac{C_{DBS}}{(1 - Hct_{\text{fixed}})}$	34	22	42	46	46	1136	53	32 (26–38)	−13 to 77	1.710	−168
Hematocrit (individual) and correction factor (patient level)	(4)	$EC_{\text{plasma}} = \frac{C_{DBS}}{(1 - Hct_{\text{individual}})} \times CF_{\text{patient}}$	28	18	46	39	39	821	44	31 (28–35)	1.9–61	1.497	−63

Table 3 (continued)

Correction strategy	Equation no.	Equation	AR (%)	*n* accept	*n* reject	MPPE (%)	MAPE (%)	RMSE (µg/L)	RMSPE (%)	Mean bias (95% CI, %)	95% LoA (%, lower–upper)	Proportional bias	Constant bias
Hematocrit (individual) and blood-to-plasma partitioning (F_p)	(2c)	$EC_{\text{plasma}} = \frac{C_{\text{pbs}}}{(1 - Hct)} \times F_p$	11	7	57	−31	31	495	33	−37 (−41 to −34)	−66 to −8.1	0.741	−28

Proportional bias and constant bias are slope and intercept estimates, respectively, from Passing–Bablok regression. Mean bias and 95% LoA are derived from Bland–Altman analysis

AR acceptance rate, *n accept* number of samples within 20% of the mean concentration, *n reject* number of samples outside ±20%, *MPPE* median percentage prediction error, *MAPE* median absolute percentage error, *CI* confidence interval, *RMSE* root mean squared error (in concentration units), *RMSPE* root mean squared percentage error, *95% LoA* 95% limits of agreement, *Hct* hematocrit, *CF* correction factor, *fu* unbound fraction, *Kbc/pl* blood cell-to-plasma concentration ratio, *poly* polynomial fit

Several literature-based strategies formed an intermediate tier (AR 83–67%). This tier comprised the Hct-adjusted polynomial correction (Eq. 3d; AR 83%), empiric multipliers using patient- or sample-level correction factors (Eq. 5a, 5b; AR 75%), and regression-based calibrations versus plasma (Eqs. 6a, 6b, 7b; AR 69–80%). Errors were low (MPPE 0.0% to +3.1%; MAPE 10–11%) with LoA up to 57%. The lowest-performing approaches included strategies based on Hct (Eqs. 3b, 3c, 2c, 4). These showed AR values as low as 2%, with MPPE and MAPE up to 51% and LoA extending beyond 60%, performing substantially worse than fitted regression models. Detailed results for all VAMS-based strategies are presented in Table 4.

3.6 Self-sampling Feasibility

Of 25 enrolled patients, 23 consented to self-microsampling (acceptance: 23/25). Among these, 21 attempted self-microsampling (performance: 21/23) with two unable to perform sampling. Of the 21 patients, 18 completed microsampling independently (independence: 18/21), while 3 required caregiver assistance. Participants were expected to return 84 device samples (42 DBS, 42 VAMS). Overall, 76% samples were deemed suitable for analysis, as assessed by the laboratory technician, and contained detectable venetoclax (sample adequacy: 64/84), with comparable adequacy for DBS and VAMS. Sample failures were attributed to DBS-insufficient capillary filling (6/10) or no capillary filling (4/10); VAMS-oversampling (5/10) or incomplete tip filling (5/10). Examples of failed DBS and VAMS samples are shown in Supplementary Fig. S3.

Usability of both microsampling devices was assessed with the ten-item SUS. Item-level SUS ratings (Fig. 4a) were consistently higher for VAMS (Mitra Clamshell) than for DBS (HemaXis DB10) across all ten direction-aligned items, which indicates greater perceived ease of use, better integration, less complexity, and higher user confidence. Consistent with these findings, the within-patient difference in total SUS scores (Fig. 4b) favored VAMS by 14 SUS points on the 0–100 scale (Hodges–Lehmann Δ; 95% CI 7.5–28; $p = 0.001$).

4 Discussion

This is the first comprehensive clinical validation study of capillary microsampling for venetoclax. We demonstrated that capillary microsampling can reliably quantify venetoclax concentrations when appropriate whole blood-to-plasma conversion is applied. Without correction, venetoclax concentrations from both DBS and VAMS underestimated plasma (mean bias −21% and −14%, respectively). This

Table 4 Performance of correction methods for estimating plasma-equivalent venetoclax concentrations from VAMS measurements. Methods are ranked by acceptance rate (percentage of samples with predicted plasma concentration within 20% of the mean concentration)

Correction strategy	Equation no.	Equation	AR (%)	*n* accept	*n* reject	MPPE (%)	MAPE (%)	RMSE (µg/L)	RMSPE (%)	Mean bias (95% CI, %)	95% LoA (%, lower-upper)	Proportional bias	Constant bias
Hematocrit-plasma/capillary ratio (linear model)	(1a)	$EC_{plasma} = C_{VAMS} x(axHct + b)$	91	58	6	−0.1	8.2	234	14	0.8 (−2.5 to 4.1)	−25 to 27	1.009	−8
Hematocrit-plasma/capillary ratio (exp model)	(1b)	$EC_{plasma} = C_{VAMS} x(axe^{(b \cdot Hct)})$	91	58	6	−0.2	8.0	232	14	0.8 (−2.5 to 4.0)	−25 to 26	1.004	−1
Hematocrit-plasma/capillary ratio (log model)	(1c)	$EC_{plasma} = C_{VAMS}\, x(ax\ln(Hct) + b)$	89	57	7	−0.7	8.7	242	14	0.8 (−2.5 to 4.2)	−26 to 27	1.017	−12
Hematocrit-plasma/capillary ratio (polynomial model)	(1d)	$EC_{plasma} = C_{VAMS} x(ax\, Hct) + bx(Hct)^2 + c)$	88	56	8	−0.6	7.8	238	13	0.8 (−2.4 to 3.9)	−24 to 26	1.004	−8
Hematocrit (individual)	(3d)	$EC_{plasma} = \frac{C_{VAMS}}{\left(1 - Hct + Hct^2\right)}$	83	53	11	8.5	11	421	19	7.5 (3.8 to 11)	−21 to 36	1.151	−53
Plasma-capillary calibration (Passing–Bablok regression)	(6b)	$EC_{plasma} = \frac{C_{VAMS} + b}{a_{VAMS\sim plasma}}$	80	51	13	0.0	11	255	17	1.2 (−2.8 to 5.1)	−30 to 32	1.000	−0
Correction factor (patient level)	(5a)	$EC_{plasma} = C_{VAMS} xCF_{patient}$	75	48	16	1.5	13	355	16	−0.4 (−4.4 to 3.6)	−32 to 31	1.108	−78
Correction factor (sample level)	(5b)	$EC_{plasma} = C_{VAMS} xCF_{sample}$	75	48	16	0.0	12	335	16	−1.9 (−5.9 to 2.1)	−34 to 30	1.091	−76
Plasma-capillary calibration (linear regression)	(7b)	$EC_{plasma} = axC_{VAMS} + b$	70	45	19	2.9	10	207	37	8.6 (2.4 to 15)	−40 to 57	0.876	144

Table 4 (continued)

Correction strategy	Equation no.	Equation	AR (%)	*n* accept	*n* reject	MPPE (%)	MAPE (%)	RMSE (µg/L)	RMSPE (%)	Mean bias (95% CI, %)	95% LoA (%, lower-upper)	Proportional bias	Constant bias
Plasma-capillary calibration (Deming regression)	(6a)	$EC_{plasma} = \frac{C_{VAMS}+b}{a_{VAMS\sim plasma}}$	69	44	20	3.1	10	208	33	7.4 (1.6 to 13)	−38 to 53	0.893	122
Plasma-capillary calibration (slope Passing–Bablok regression)	(6c)	$EC_{plasma} = \frac{C_{VAMS}}{a_{VAMS\sim plasma}}$	67	43	21	−8.3	14	258	17	−11 (−15 to −6.5)	−42 to 21	1.000	−70
Plasma-capillary calibration (slope linear regression)	(7a)	$EC_{plasma} = \frac{C_{VAMS}}{a_{VAMS\sim plasma}}$	64	41	23	−12	14	249	19	−14 (−18 to −10)	−46 to 17	0.963	−67
No correction strategy	–	–	58	37	27	−14	16	255	20	−17 (−21 to −13)	−49 to 14	0.933	−65
Hematocrit (mean)	(3b)	$EC_{plasma} = \frac{C_{VAMS}}{\left(1 - Hct_{mean}\right)}$	41	26	38	31	31	858	37	25 (21–29)	−6.1 to 56	1.439	−106
Hematocrit (individual)	(3a)	$EC_{plasma} = \frac{C_{VAMS}}{\left(1 - Hct_{individual}\right)}$	38	24	40	27	27	861	37	26 (23–29)	0.5–51	1.270	−1
Hematocrit (individual) and blood-plasma partitioning ($\rho \times f_u$)	(2a)	$EC_{plasma} = \frac{C_{VAMS}}{(1 - Hct) + Hct_{individual} x \rho x f_u}$	38	24	40	27	27	624	36	26 (23–29)	0.7–51	1.273	−1
Hematocrit (individual) and blood-plasma partitioning (Kbc/pla)	(2b)	$EC_{plasma} = \frac{C_{VAMS}}{(1 - Hct) + K\frac{bc}{pla} x Hct_{individual}}$	38	24	40	27	27	628	36	26 (23–29)	0.5–51	1.270	−1
Hematocrit (individual) and blood-to-plasma partitioning (F_p)	(2c)	$EC_{plasma} = \frac{C_{VAMS}}{(1 - Hct)} x F_p$	19	12	52	−28	28	439	27	−30 (−33 to −27)	−55 to −4.6	0.721	3

Table 4 (continued)

Correction strategy	Equation no.	Equation	AR (%)	*n* accept	*n* reject	MPPE (%)	MAPE (%)	RMSE (µg/L)	RMSPE (%)	Mean bias (95% CI, %)	95% LoA (%, lower–upper)	Proportional bias	Constant bias
Hematocrit (fixed)	(3c)	$EC_{plasma} = \frac{C_{VAMS}}{(1 - Hct_{fixed})}$	11	7	57	51	51	1242	57	39 (36–43)	9.7–69	1.639	− 91
Hematocrit (individual) and correction factor (patient level)	(4)	$EC_{plasma} = \frac{C_{VAMS}}{(1 - Hct_{individual})} xCF_{mean}$	2	1	63	51	51	1037	59	42 (39–45)	18–67	1.508	− 2

Proportional bias and constant bias are slope and intercept estimates, respectively, from Passing–Bablok regression. Mean bias and 95% LoA are derived from Bland–Altman analysis

AR acceptance rate, *n accept* number of samples within 20% of the mean concentration, *n reject* number of samples outside ±20%, *MPPE* median percentage prediction error, *MAPE* median absolute percentage error, *CI* confidence interval, *RMSE* root mean squared error (in concentration units), *RMSPE* root mean squared percentage error, *95% LoA* 95% limits of agreement, *HCT* hematocrit, *CF* correction factor, f_u unbound fraction, *Kbc/pl* blood cell-to-plasma concentration ratio, *poly* polynomial fit

bias was strongly linked to Hct, with higher levels causing greater underestimation of venetoclax in capillary whole blood, due to the smaller plasma fraction relative to erythrocytes. Importantly, despite both being volumetric capillary microsampling techniques, DBS (with HemaXis DB10) and VAMS (with Mitra Clamshell) differed in their Hct dependence: the venetoclax plasma/DBS concentration ratio rose steeply with increasing Hct (slope 3.52; $R^2 = 0.71$), whereas the plasma/VAMS ratio showed a more modest Hct dependence (slope 1.51; $R^2 = 0.37$). Consequently, Hct inflated the plasma/DBS ratio more than twice as strongly as plasma/VAMS, making DBS more susceptible to Hct-related bias. Using the observed relationship between Hct and the plasma-to-microsample ratio, we derived a linear correction model that achieved excellent agreement with venous plasma (AR 95% DBS, 91% VAMS), with Bland–Altman limits within the ± 25% predefined clinical threshold, no proportional or constant bias, and strong predictive performance (MPPE ≈ 0, MAPE < 15%). This fulfills international validation criteria for microsampling in PK monitoring [19, 40]. A key limitation, however, is that this approach remains dependent on contemporaneous Hct values, which are not routinely available in home-based self-sampling. This was illustrated by the few out-of-range cases in both DBS and VAMS, all traced to a single patient whose Hct was measured ≥ 20 days from sampling. Even with a low CV, stale values undermined correction accuracy. Although Hct variability was summarized descriptively using a 1-year CV to reflect real-world Hct fluctuations during treatment, our findings suggest that the timing of the Hct measurement relative to sampling is more critical for correction accuracy than long-term variability. Reliable correction to plasma therefore requires Hct measured closest to sampling. Although volumetric microsampling is often proposed to nullify technical Hct bias by standardizing sample volume [45], our findings demonstrate that physiological Hct bias persists across volumetric devices, showing that Hct remains a critical determinant. Encouragingly, recent advances in nondestructive Hct measurement for DBS and VAMS, using reflectance, near-infrared spectroscopy, or image analysis, now enable direct Hct determination from the microsample itself [46–48]. These developments may overcome one of the main barriers to routine and home-based implementation.

While our empirical Hct-ratio models (Eqs. 1a–1d) achieved excellent agreement and predictive performance, literature-based capillary blood-to-plasma correction strategies achieved only moderate-to-poor agreement, with acceptance rates typically ≤ 67% within ± 20% of plasma values and in some cases performing worse than no correction. Although venetoclax is confined to the plasma compartment [5], theory-driven Hct formulas systematically mis-corrected plasma concentrations. In DBS, dividing by (1-Hct) or applying fixed/mean Hct values consistently

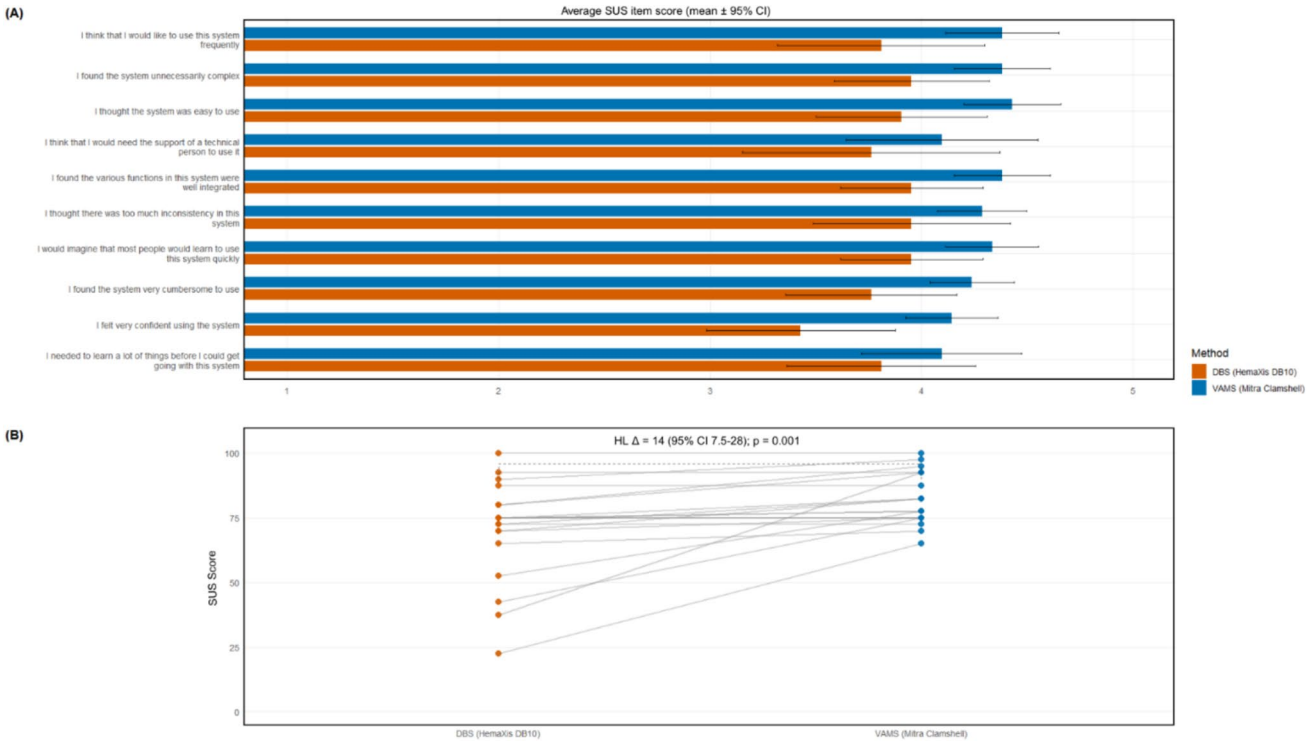

Fig. 4 System Usability Scale comparison of microsampling devices. (**a**) Item-level SUS ratings (1–5) displayed as means with 95% CIs for DBS (HemaXis DB10; orange) and VAMS (Mitra Clamshell; blue). Negatively worded items were reverse-coded so that higher values reflect better usability. (**b**) Paired dot plot of total SUS scores (0–100) linking each participant's DBS and VAMS ratings. The annotation reports the Hodges–Lehmann within-patient difference (Δ = 14; 95% CI 7.5–28; $p = 0.001$). *SUS* System Usability Scale, *DBS* dried blood spot, *VAMS* volumetric absorptive microsampling, *HL Δ* Hodges–Lehmann median paired difference, *CI* confidence interval

overestimated plasma levels, with AR values < 53% and biases exceeding 20–30%. Adding partition parameters did not improve performance. In VAMS, Hct formulas again under- or over-corrected concentrations, with only one method meeting the 67%/20% criterion, but performing suboptimally in DBS. Together, these findings demonstrate that Hct must be modeled empirically rather than through generic corrections, and consistent with prior studies, confirm that Hct alone does not explain all capillary-venous variability [25, 49].

Despite both being volumetric devices, VAMS achieved acceptable agreement and predictive performance with a broader range of literature-based strategies than DBS. In VAMS, several regression-based calibrations and conversion factors crossed the 67% AR threshold (69–80%) with low-to-moderate bias and MAPE around 10–13%. However, their 95% LoA still extended up to −40% to 57%, exceeding the ±25% clinical target. In contrast, no literature-based correction strategy in DBS met the 67%/20% acceptability criterion, with the best-performing approaches plateauing at 61–62% AR and MAPE 15–17%. Even when mean bias was small, variability dominated. Overall, wide 95% LoA for both devices limited the clinical acceptability of all literature-based correction strategies.

Reviewing the outcomes of literature-based correction strategies summarized in Table 1 reveals substantial heterogeneity that limits comparability across studies. Many did not meet IATDMCT recommendations of ≥ 40 paired samples spanning the full therapeutic range [19, 40], with several relying on small cohorts or restricted to trough levels, which can inflate apparent accuracy while masking error at higher concentrations, as would be relevant for peak or AUC-based TDM. Definitions of acceptability also varied, with AR thresholds ranging from 15 to 25% and reference values differing (plasma versus mean), while predictive metrics were often not reported. Methodological diversity was considerable: some studies used venous rather than capillary blood, non-volumetric punch DBS instead of volumetric devices, and applied different regression approaches (slope-only factors, ordinary least squares, Deming, Passing–Bablok). Hct handling was likewise inconsistent, often relying on fixed or mean values or population-level partition parameters instead of contemporaneous, sample-level Hct. Another often overlooked factor is the timing of paired sample collection, which should occur within 5–10 min [19] and has been reported as challenging in clinical practice [49]. Even small deviations can introduce variability in the post-dose window until Tmax or at trough depending

on the drug's half-life. In our study, the 10-min window for paired sampling was not feasible in four cases. Together, these differences may help explain why strategies developed for other plasma-confined drugs did not yield similar results for venetoclax, and more broadly confirm that performance does not generalize across drugs, devices, or cohorts.

As an alternative for plasma-confined drugs, dried plasma spots have been explored to bypass whole blood-to-plasma conversion, supported by the emergence of devices that generate dried plasma spots directly from a capillary drop. However, they often require relatively large blood volumes and show inconsistent analyte recovery, including reduced plasma protein recovery, which is a significant limitation for highly protein-bound compounds [40]. Systematic errors have also been reported when comparing dried plasma spots with liquid plasma for oncolytic drugs [50], underscoring the need for further bioanalytical and clinical validation before DPS can replace DBS or VAMS in this setting.

In addition to clinical validation, we evaluated feasibility, as clinical implementation requires methods suitable for routine care. We demonstrated that home-based self-sampling was feasible: nearly all patients collected microsamples independently, most returned samples were analytically adequate (76%), and usability ratings favored VAMS over DBS as the more patient-friendly option for decentralized venetoclax monitoring. Comparable findings have been reported in kidney transplant recipients, where both DBS and VAMS proved feasible, with a consistent end-user preference for VAMS [51]. From a laboratory perspective, however, DBS cards such as the HemaXis DB10 integrate readily into automated workflows, whereas VAMS automation remains less developed [52]. Similar feasibility has been reported in other oncology cohorts using VAMS, with successful home-sampling rates ranging from 70 to 93% across studies involving oral oncolytics [49, 53]. In contrast, self-sampling feasibility data for DBS using the HemaXis DB10 device remain limited in oncology. However, a real-world study in kidney transplant recipients reported that 91% of returned samples were suitable for analysis [51]. It is important to interpret home feasibility outcomes within the clinical context, as populations differ markedly. For example, venetoclax-treated patients with AML face a limited life expectancy and are generally more fragile [54], whereas kidney transplant recipients often achieve long-term survival [55]. Training conditions also differed between the VAMS home-sampling studies: in one study, patients relied mainly on written instructions after in-clinic demonstration [53], whereas in another, initial sampling was supervised and instructions reinforced [49]. In our study, initial sampling was also unsupervised, further suggesting that structured training could improve outcomes. Broader comparisons of microsampling devices confirm device-dependent feasibility, with success rates of 65–89% for various microsampling devices, but only 12% for the high-volume device Minicollect tube [20]. It is also important to acknowledge that remote monitoring with these devices will not be feasible for all patients. In our study, SUS scores ranged as low as 23 for DBS and 65 for VAMS, indicating variability in user acceptance. Although sample adequacy was analytically acceptable, the 24% failure rate in our study remains substantial. This may have operational implications: delayed throughput times, repeat sampling, and additional patient contacts may offset some of the logistical advantages of home-based microsampling and influence overall financial feasibility. Therefore, microsampling should not be considered a one-to-one replacement for venipuncture in all patients. Instead, structured training and careful patient selection, including identifying individuals unlikely to perform microsampling independently, will be critical for successful implementation.

Microsampling may be particularly attractive in outpatient settings such as CLL, where venetoclax treatment often occurs in the ambulatory setting and long-term monitoring is required. This reflects the more favorable prognosis and longer survival observed in CLL compared with AML [56]. In contrast, venetoclax-treated patients with AML require intensive in-hospital treatment and monitoring and are at higher risk for infection-related complications [3]. Although these patients already visit the hospital frequently, minimizing avoidable exposure remains clinically relevant [57]. In this context, home-based microsampling could enable more intensive PK profiling, such as AUC assessment, without additional clinic visits. Importantly, although this study provides clinical validation and demonstrates feasibility, the clinical utility of venetoclax microsampling remains to be studied.

This study has some limitations. First, although we included 25 participants and 64 paired samples, meeting the IATDMCT threshold of ≥ 25 patients and ≥ 40 samples when patient numbers are limited, this remains below the general recommendation of ≥ 40 participants with single paired samples [19]. Nonetheless, our sample size was higher than most previous oncolytic drug studies using microsampling (Table S1). Second, we did not validate the conversion formula in an independent dataset. Only one prior study ($n = 12$ patients) among those whose correction strategies we applied in this study reported validation in an independent sample set [35]. This limitation is particularly relevant for general correction factors and regression-based calibrations, which are more prone to overfitting [25]. In contrast, our primary approach was individualized, using the empirically observed Hct-plasma/microsample ratio, which may be less sensitive to this issue. Third, while patients successfully performed home-based sampling, they were not instructed to collect trough samples specifically; feasibility for clinically relevant timepoints such as troughs therefore remains to be demonstrated. Finally, patients were not

randomly selected but represented venetoclax-treated individuals at our center who were clinically able and willing to participate. This introduces potential self-selection bias, as fitter or more functionally independent patients may have been overrepresented, which could have led to an overestimation of feasibility outcomes. At the same time, the study has notable strengths. Sampling covered both trough and a wide range of post-dose intervals, capturing pharmacokinetic variability across the therapeutic range. This design allowed for evaluation of suitability not only for trough-based monitoring, but also for peak- or AUC-based TDM. Two volumetric devices were evaluated, which are better suited for home use and circumvent key limitations of non-volumetric microsampling [19, 45]. Analyzing both also revealed device-specific differences often overlooked when microsampling techniques are considered interchangeable. Finally, we systematically evaluated a broad set of correction strategies, including those previously proposed for plasma-confined drugs, which provided important insights into the conditions under which correction approaches succeed or fail.

5 Conclusions

Accurate venetoclax quantification from capillary microsamples was achievable when individualized hematocrit-based plasma conversion was applied, with both DBS and VAMS meeting international validation criteria. Literature-based whole-blood-to-plasma correction strategies performed inconsistently, underscoring the need for drug-, device-, and population-specific calibration. Home-based self-microsampling was feasible, with a modest patient preference for VAMS. Future studies should prioritize independent validation, reduction of preanalytical errors, integration of nondestructive contemporaneous Hct measurement for both VAMS and DBS, and structured patient training to improve success rates and support broader clinical implementation of microsampling for venetoclax.

Supplementary Information The online version contains supplementary material available at https://doi.org/10.1007/s40262-026-01635-3.

Funding Open access funding provided by Leiden University Medical Center (LUMC). This work did not receive any financial support. The authors received no financial support for the research and/or publication of this article.

Declarations

Conflict of interest Dirk Jan Moes is an editorial board member of *Clinical Pharmacokinetics*. He was not involved in the selection of peer reviewers for the manuscript or any of the subsequent editorial decisions. Jesse Swen has received lecture fees from Lundbeck, paid directly to his employer (Leiden University Medical Center). The other authors declare that they have no competing interests.

Data availability statement All analyses underlying the conclusions are described in the article and its Supplementary Materials. Owing to institutional and ethical restrictions, the datasets generated and/or analyzed in this study are not publicly available; deidentified datasets and the analysis can be obtained from the corresponding author on reasonable request. Scripts were developed in a Dutch clinical context and contain both Dutch- and English-language elements, reflecting the original data structure.

Ethics approval This study was approved by the institutional review board of Leiden University Medical Center (approval number: NL86162.058.24). All procedures were conducted in accordance with the ethical standards of the Declaration of Helsinki.

Consent to participate Informed consent was obtained from all individual participants included in the study.

Consent for publication Not applicable.

Author contributions Concept and design: D.J.A.R.M. and A.D.L.; acquisition of data: J.R., A.D.L., A.A., and P.vdB.; formal analysis and visualization: A.D.L. and J.R.; methodology and validation: A.D.L., D.J.A.R.M., E.M., J.R., and J.J.S; Project administration: J.R., A.D.L., and E.M.; supervision: D.J.A.R.M. and J.J.S; writing—original draft: A.D.L; review and editing: A.D.L., D.J.A.R.M., A.A., E.M., J.R., P.vdB, and J.J.S. All authors read and approved the final manuscript.

References

1. Lasica M, Anderson MA. Review of venetoclax in CLL, AML and multiple myeloma. J Pers Med. 2021. https://doi.org/10.3390/jpm11060463.
2. Agency EM: Venclyxto (venetoclax) summary of product characteristics. 2023. https://www.ema.europa.eu/en/medicines/human/EPAR/venclyxto. Accessed 13 Mar 2025.
3. Waggoner M, Katsetos J, Thomas E, Galinsky I, Fox H. Practical management of the venetoclax-treated patient in chronic lymphocytic leukemia and acute myeloid leukemia. J Adv Pract Oncol. 2022;13(4):400–15. https://doi.org/10.6004/jadpro.2022.13.4.4.
4. Kt MF, Semwal M, Yoosuf BT, Lad D, Bansal D. Venetoclax adverse event monitoring: a safety meta-analysis of randomized controlled trials and a retrospective evaluation of the FAERS. Ann Hematol. 2024;103(8):3179–91. https://doi.org/10.1007/s00277-024-05676-1.
5. Research CfDEa. Clinical pharmacology and biopharmaceutics review: NDA 208573 venetoclax. Silver Spring: U.S. Food and Drug Administration; 2016.

6. Philippe M, Guitton J, Goutelle S, Thoma Y, Favier B, Chtiba N, et al. Pharmacokinetic consideration of venetoclax in acute myeloid leukemia patients: a potential candidate for TDM? A short communication. Ther Drug Monit. 2024;46(1):127–31. https://doi.org/10.1097/ftd.0000000000001151.
7. Kobayashi M, Yasu T, Suzaki K, Kosugi N. Utility of therapeutic drug monitoring of venetoclax in acute myeloid leukemia. Med Oncol. 2022;39(12):259. https://doi.org/10.1007/s12032-022-01865-y.
8. Salem AH, Menon RM. Clinical pharmacokinetics and pharmacodynamics of venetoclax, a selective B-cell lymphoma-2 inhibitor. Clin Transl Sci. 2024;17(5):e13807. https://doi.org/10.1111/cts.13807.
9. Zhao Y, Guo N, Zhu Y, Shang J, Chen J, Luo X, et al. Population pharmacokinetic models of venetoclax in hematologic malignancies: a systematic review. Drug Des Dev Ther. 2024;18:1771–84. https://doi.org/10.2147/dddt.S458927.
10. Agarwal SK, DiNardo CD, Potluri J, Dunbar M, Kantarjian HM, Humerickhouse RA, et al. Management of venetoclax-posaconazole interaction in acute myeloid leukemia patients: evaluation of dose adjustments. Clin Ther. 2017;39(2):359–67. https://doi.org/10.1016/j.clinthera.2017.01.003.
11. Administration USFaD: VENCLEXTA (venetoclax) prescribing information. 2019. https://www.accessdata.fda.gov/drugsatfda_docs/label/2019/208573s013lbl.pdf. Accessed 17 Mar 2025.
12. Nederland SH-OvV: a trial to assess cobicistat boosted venetoclax in combination with azacitidine in adult patients with newly diagnosed AML (HO171). 2024. https://clinicaltrials.gov/study/NCT06014489?term=HO171%20AML&rank=1. Accessed.
13. Westra N, Touw D, Lub-de Hooge M, Kosterink J, Oude Munnink T. Pharmacokinetic boosting of kinase inhibitors. Pharmaceutics. 2023. https://doi.org/10.3390/pharmaceutics15041149.
14. Mueller-Schoell A, Groenland SL, Scherf-Clavel O, van Dyk M, Huisinga W, Michelet R, et al. Therapeutic drug monitoring of oral targeted antineoplastic drugs. Eur J Clin Pharmacol. 2021;77(4):441–64. https://doi.org/10.1007/s00228-020-03014-8.
15. Wilhelm AJ, den Burger JCG, Swart EL. Therapeutic drug monitoring by dried blood spot: progress to date and future directions. Clin Pharmacokinet. 2014;53(11):961–73. https://doi.org/10.1007/s40262-014-0177-7.
16. Avvisati G, Tirindelli MC, Annibali O. Thrombocytopenia and hemorrhagic risk in cancer patients. Crit Rev Oncol Hematol. 2003;48:S13–6. https://doi.org/10.1016/j.critrevonc.2003.04.001.
17. Zailani NNB, Ho PC. Dried blood spots-a platform for therapeutic drug monitoring (TDM) and drug/disease response monitoring (DRM). Eur J Drug Metab Pharmacokinet. 2023;48(5):467–94. https://doi.org/10.1007/s13318-023-00846-4.
18. Meertens M, Rosing H, Steeghs N, Beijnen JH, Huitema ADR. Advancing therapeutic drug monitoring for oral targeted anticancer drugs: from hospital-based towards home-sampling. Biomed Chromatogr. 2025;39(5):e70056. https://doi.org/10.1002/bmc.70056.
19. Capiau S, Veenhof H, Koster RA, Bergqvist Y, Boettcher M, Halmingh O, et al. Official International Association for Therapeutic Drug Monitoring and Clinical Toxicology guideline: development and validation of dried blood spot-based methods for therapeutic drug monitoring. Ther Drug Monit. 2019;41(4):409–30. https://doi.org/10.1097/ftd.0000000000000643.
20. Boffel L, Van Mensel A, Pauwels J, Den Hond E, Bessems J, Van Uytfanghe K, et al. Self-sampling by adolescents at home: assessment of the feasibility to successfully collect blood microsamples by inexperienced individuals. AAPS J. 2024;26(4):75. https://doi.org/10.1208/s12248-024-00947-1.
21. LUMC: Medicijnmeting thuis via een vingerprik afname: dried blood spot (DBS). 2025. https://www.lumc.nl/afdelingen/klinisch-chemisch-laboratorium/overige-folders/medicijnmeting-thuis-via-een-vingerprik-afname-dried-blood-spot-dbs/. Accessed 17 July 2025.
22. EMA. 2025. https://www.ema.europa.eu/en/documents/product-information/venclyxto-epar-product-information_en.pdf. Accessed 17 July 2025.
23. Salem AH, Agarwal SK, Dunbar M, Enschede SL, Humerickhouse RA, Wong SL. Pharmacokinetics of venetoclax, a novel BCL-2 inhibitor, in patients with relapsed or refractory chronic lymphocytic leukemia or non-Hodgkin lymphoma. J Clin Pharmacol. 2017;57(4):484–92. https://doi.org/10.1002/jcph.821.
24. ICH: ICH guideline M10 on bioanalytical method validation and study sample analysis. 2023. https://www.ema.europa.eu/en/documents/scientific-guideline/ich-guideline-m10-bioanalytical-method-validation-step-5_en.pdf. Accessed 17 July 2025.
25. Iacuzzi V, Posocco B, Zanchetta M, Gagno S, Poetto AS, Guardascione M, et al. Dried blood spot technique applied in therapeutic drug monitoring of anticancer drugs: a review on conversion methods to correlate plasma and dried blood spot concentrations. Pharm Res. 2021;38(5):759–78. https://doi.org/10.1007/s11095-021-03036-6.
26. Boons C, Chahbouni A, Schimmel AM, Wilhelm AJ, den Hartog YM, Janssen J, et al. Dried blood spot sampling of nilotinib in patients with chronic myeloid leukaemia: a comparison with venous blood sampling. J Pharm Pharmacol. 2017;69(10):1265–74. https://doi.org/10.1111/jphp.12757.
27. Jager NG, Rosing H, Schellens JH, Beijnen JH, Linn SC. Use of dried blood spots for the determination of serum concentrations of tamoxifen and endoxifen. Breast Cancer Res Treat. 2014;146(1):137–44. https://doi.org/10.1007/s10549-014-2999-2.
28. Nijenhuis CM, Huitema AD, Marchetti S, Blank C, Haanen JB, van Thienen JV, et al. The use of dried blood spots for pharmacokinetic monitoring of vemurafenib treatment in melanoma patients. J Clin Pharmacol. 2016;56(10):1307–12. https://doi.org/10.1002/jcph.728.
29. Antunes MV, Raymundo S, Wagner SC, Mattevi VS, Vieira N, Leite R, et al. DBS sampling in imatinib therapeutic drug monitoring: from method development to clinical application. Bioanalysis. 2015;7(16):2105–17. https://doi.org/10.4155/bio.15.101.
30. Hahn RZ, Arnhold PC, Andriguetti NB, Schneider A, Klück HM, Dos Reis SL, et al. Determination of irinotecan and its metabolite SN-38 in dried blood spots using high-performance liquid-chromatography with fluorescence detection. J Pharm Biomed Anal. 2018;150:51–8. https://doi.org/10.1016/j.jpba.2017.11.079.
31. Andriguetti NB, Hahn RZ, Lizot LF, Raymundo S, Costa JL, da Cunha KF, et al. Analytical and clinical validation of a dried blood spot assay for the determination of paclitaxel using high-performance liquid chromatography-tandem mass spectrometry. Clin Biochem. 2018;54:123–30. https://doi.org/10.1016/j.clinbiochem.2018.02.020.
32. Raymundo S, Muller VV, Andriguetti NB, Tegner M, Artmann AC, Kluck HM, et al. Determination of docetaxel in dried blood spots by LC-MS/MS: method development, validation and clinical application. J Pharm Biomed Anal. 2018;157:84–91. https://doi.org/10.1016/j.jpba.2018.05.011.
33. Kralj E, Trontelj J, Pajič T, Kristl A. Simultaneous measurement of imatinib, nilotinib and dasatinib in dried blood spot by ultra high performance liquid chromatography tandem mass spectrometry. J Chromatogr B Analyt Technol Biomed Life Sci. 2012;903:150–6. https://doi.org/10.1016/j.jchromb.2012.07.011.
34. Režonja Kukec R, Grabnar I, Mrhar A, Čebron Lipovec N, Čufer T, Vovk T. A simple dried blood spot method for clinical pharmacological analyses of etoposide in cancer patients using liquid chromatography and fluorescence detection. Clin Chim Acta. 2016;452:99–105. https://doi.org/10.1016/j.cca.2015.10.026.

35. Iacuzzi V, Posocco B, Zanchetta M, Montico M, Marangon E, Poetto AS, et al. Development and validation of LC-MS/MS method for imatinib and norimatinib monitoring by finger-prick DBS in gastrointestinal stromal tumor patients. PLoS ONE. 2019;14(11):e0225225. https://doi.org/10.1371/journal.pone.0225225.
36. de Wit D, den Hartigh J, Gelderblom H, Qian Y, den Hollander M, Verheul H, et al. Dried blood spot analysis for therapeutic drug monitoring of pazopanib. J Clin Pharmacol. 2015;55(12):1344–50. https://doi.org/10.1002/jcph.558.
37. Lee J, Jung SY, Choi MY, Park JS, Park SK, Lim SA, et al. Development of a dried blood spot sampling method towards therapeutic monitoring of radotinib in the treatment of chronic myeloid leukaemia. J Clin Pharm Ther. 2020;45(5):1006–13. https://doi.org/10.1111/jcpt.13124.
38. Antunes MV, Raymundo S, de Oliveira V, Staudt DE, Gössling G, Peteffi GP, et al. Ultra-high performance liquid chromatography tandem mass spectrometric method for the determination of tamoxifen, N-desmethyltamoxifen, 4-hydroxytamoxifen and endoxifen in dried blood spots--development, validation and clinical application during breast cancer adjuvant therapy. Talanta. 2015;132:775–84. https://doi.org/10.1016/j.talanta.2014.10.040.
39. Verheijen RB, Bins S, Thijssen B, Rosing H, Nan L, Schellens JH, et al. Development and clinical validation of an LC-MS/MS method for the quantification of pazopanib in DBS. Bioanalysis. 2016;8(2):123–34. https://doi.org/10.4155/bio.15.235.
40. Boffel L, De Baets H, Heughebaert L, Rispens T, Åsberg A, Shipkova M, et al. To convert or not to convert? Official International Association of Therapeutic Drug Monitoring and Clinical Toxicology guideline: considerations and recommendations for converting capillary blood microsampling concentrations to plasma concentrations. Ther Drug Monit. https://doi.org/10.1097/FTD.0000000000001393.
41. Passing H, Bablok. A new biometrical procedure for testing the equality of measurements from two different analytical methods. Application of linear regression procedures for method comparison studies in clinical chemistry, Part I. J Clin Chem Clin Biochem. 1983;21(11):709–20. https://doi.org/10.1515/cclm.1983.21.11.709.
42. Bland JM, Altman DG. Statistical methods for assessing agreement between two methods of clinical measurement. Lancet. 1986;1(8476):307–10.
43. (Australia) TGA. AusPAR Attachment 2: Extract from the Clinical Evaluation Report for Venetoclax (Venclexta). Commonwealth of Australia; 2016.
44. Brooke J. SUS: a retrospective. J Usability Stud. 2013;8(2):29–40.
45. Velghe S, Delahaye L, Stove CP. Is the hematocrit still an issue in quantitative dried blood spot analysis? J Pharm Biomed Anal. 2019;163:188–96. https://doi.org/10.1016/j.jpba.2018.10.010.
46. Luginbühl M, Gaugler S. Addressing new possibilities and new challenges: automated nondestructive hematocrit normalization for dried blood spots. Ther Drug Monit. 2021. https://doi.org/10.1097/FTD.0000000000000887.
47. Heughebaert L, Boffel L, Lühr C, Lambrecht S, Stove CP. Near-infrared-based hematocrit determination of dried blood samples collected by volumetric absorptive microsampling: an in-depth evaluation. Microchem J. 2024;205:111330. https://doi.org/10.1016/j.microc.2024.111330.
48. Daousani C, Kostić N, Malenović A, Rmandić M, Dotsikas Y. On the use of image analysis for hematocrit evaluation in dried blood spots. Appl Sci Basel. 2024;14(21):9860.
49. Zimmermann S, Aghai-Trommeschlaeger F, Kraus S, Grigoleit GU, Gesierich A, Schilling B, et al. Clinical validation and assessment of feasibility of volumetric absorptive microsampling (VAMS) for monitoring of nilotinib, cabozantinib, dabrafenib, trametinib, and ruxolitinib. J Pharm Biomed Anal. 2023;228:115311. https://doi.org/10.1016/j.jpba.2023.115311.
50. Mukai Y, Yoshida Y, Yoshida T, Kondo T, Inotsume N, Toda T. Simultaneous quantification of BCR-ABL and Bruton tyrosine kinase inhibitors in dried plasma spots and its application to clinical sample analysis. Ther Drug Monit. 2021;43(3):386–93. https://doi.org/10.1097/ftd.0000000000000825.
51. Zwart TC, Metscher E, van der Boog PJM, Swen JJ, de Fijter JW, Guchelaar HJ, et al. Volumetric microsampling for simultaneous remote immunosuppressant and kidney function monitoring in outpatient kidney transplant recipients. Br J Clin Pharmacol. 2022;88(11):4854–69. https://doi.org/10.1111/bcp.15433.
52. Delahaye L, Veenhof H, Koch BCP, Alffenaar J-WC, Linden R, Stove C. Alternative sampling devices to collect dried blood microsamples: state-of-the-art. Ther Drug Monit. 2021. https://doi.org/10.1097/FTD.0000000000000864.
53. Meertens M, Kerssemakers N, de Vries N, Rosing H, Steeghs N, Beijnen JH, et al. Clinical application of volumetric absorptive microsampling for therapeutic drug monitoring of oral targeted anticancer drugs. Ther Drug Monit. 2025. https://doi.org/10.1097/ftd.0000000000001315.
54. Hu M, Li W, Zhang Y, Liang C, Tan J, Wang Y. Venetoclax in adult acute myeloid leukemia. Biomed Pharmacother. 2023;168:115820. https://doi.org/10.1016/j.biopha.2023.115820.
55. Hariharan S, Israni AK, Danovitch G. Long-term survival after kidney transplantation. N Engl J Med. 2021;385(8):729–43. https://doi.org/10.1056/NEJMra2014530.
56. Kantarjian HM, Jain N, Garcia-Manero G, Welch MA, Ravandi F, Wierda WG, et al. The cure of leukemia through the optimist's prism. Cancer. 2022;128(2):240–59. https://doi.org/10.1002/cncr.33933.
57. Baden LR, Swaminathan S, Almyroudis NG, Angarone M, Baluch A, Barros N, et al. Prevention and treatment of cancer-related infections, Version 3.2024, NCCN Clinical Practice Guidelines in Oncology. J Natl Compr Canc Netw. 2024;22(9):617–44. https://doi.org/10.6004/jnccn.2024.0056.